CHEMISTRY OF MATERIALS

Article

pubs.acs.org/cm

Designing Fluorescent Peptide Sensors with Dual Specificity for the Detection of HIV-1 Protease

Karla-Luise Herpoldt,[†] Arbel Artzy-Schnirman,[†] Andrew J. Christofferson,[‡] Adam J. Makarucha,[‡] Roberto de la Rica,[†,§] Irene Yarovsky,*[,‡] and Molly M. Stevens*[,†]

[†]Department of Materials, Department of Bioengineering, Institute of Biomedical Engineering, Imperial College London, Prince Consort Road, London SW7 2AZ, United Kingdom

[‡]Health Innovations Research Institute, RMIT University, GPO Box 2476, Melbourne, Victoria 3001, Australia

Supporting Information

ABSTRACT: HIV-1 protease is a key enzyme in the life cycle of HIV/AIDS, as it is responsible for the formation of the mature virus particle. We demonstrate here that phage-display peptides raised against this enzyme can be used as peptide sensors for the detection of HIV-1 protease in a simple, one-pot assay. The presence of the enzyme is detected through an energy transfer between two peptide sensors when simultaneously complexed with the target protein. The multivalent nature of this assay increases the specificity of the detection by requiring all molecules to be interacting in order for there to be a FRET signal. We also perform molecular dynamics simulations to explore the interaction between the protease and the peptides in order to guide the design of these peptide sensors and to understand the mechanisms which cause these simultaneous binding events. This approach aims to facilitate the development of new assays for enzymes that are not dependent on the cleavage of a substrate and do not require multiple washing steps.

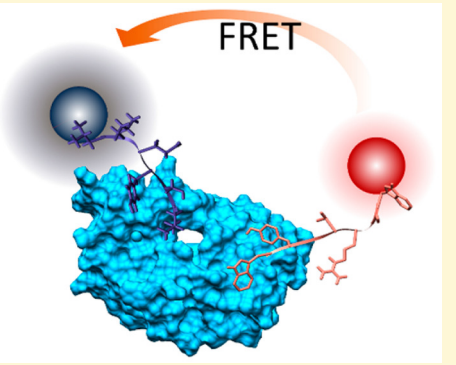

INTRODUCTION

Human immunodeficiency virus type 1 (HIV-1) is the most common cause of acquired immune deficiency syndrome (AIDS) worldwide, with some 2.1 million new cases being diagnosed in 2013.[1] HIV-1 protease (HIV-1 PR) is a dimeric enzyme from the family of aspartic proteases. It is a crucial enzyme in the lifecycle of the HIV virion, being responsible for the cleavage of the precursor polyproteins into the mature virus particle.[2] The virus remains ineffective without the presence of an active form of this enzyme, leading it to be considered as the major clinical target for antiretroviral therapies.[3] Although it has been widely exploited as a drug target and exhibits broad substrate recognition, only a few studies document the use of the enzyme as a biomarker for HIV infection.[4−7] While these methods report detection limits in the low picomolar range (LOD < 1 pM), they are limited in their effectiveness as point-of-care diagnostics given their reliance on detection mechanisms involving complex instrumentation such as surface plasmon resonance (SPR) or quartz crystal microbalance (QCM). Furthermore, in these approaches the signal is generated by the cleavage of a peptide substrate by the HIV-1 PR, and therefore, they are also susceptible to false positives, since the peptides could be cleaved nonspecifically by other proteases.

Traditional HIV diagnostics are divided into three main categories: those which detect the patient's antibodies against HIV, those which detect the p24 antigen, and those which rely on RT-PCR for the detection of viral load DNA.[8] While these techniques are highly sensitive, they too suffer from the requirements of expensive equipment and reagents as well as highly skilled, laboratory-trained staff, making it unsuitable for use in resource-limited settings. A full discussion of HIV diagnostic tools is beyond the scope of this Article, but comprehensive reviews can be found by Suaifan et al.[9] and Cornett and Kirn.[10]

Förster resonance energy transfer (FRET) has long been used as a tool to study active enzymes, in particular, proteases.[11] We have previously reported the use of FRET to detect the presence of disease related enzymes in serum.[12,13] In these studies the single event that is monitored is the cleavage of a peptide tagged with a pair of fluorescent FRET probes. The peptide acts as the substrate for the enzyme of interest so that in the presence of the enzyme the peptide is cleaved and the FRET disappears. FRET is well-suited for this detection as energy transfer will only occur between two nonradiatively coupled fluorophores if they are within 10 nm of each other, allowing detection from a single recognition event to occur. However, this same advantage can limit the complexity of systems that can be studied since the detection probe must be carefully designed to enable an efficient signal. Due to the strong distance dependence on energy transfer efficiency (r^6), it can be challenging to design an enzyme substrate that is short

Received: September 17, 2015
Revised: September 24, 2015

DOI: 10.1021/acs.chemmater.5b03651
Chem. Mater. XXXX, XXX, XXX−XXX

enough to fall within this range but long enough to be resistant to nonspecific cleavage.

Herein we describe a FRET-based method of detection of HIV-1 protease using multiple recognition elements which does not rely on peptide cleavage (Figure 1). These peptide sensors

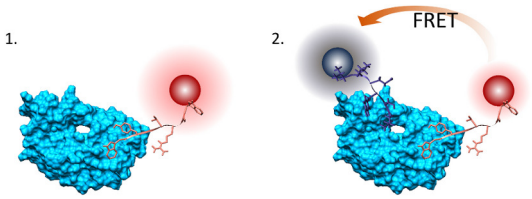

Figure 1. Schematic of the detection mechanism of HIV-1 protease. (1) A fluorescent nanosensor binds specifically to the HIV-1 PR molecule (peptide nanosensor 1 WSRVGYW-AF647). (2) A second nanosensor (peptide nanosensor 2 LLEYSL-BHQ-3), tagged with a fluorescent quencher, interacts with the active site of the protease. The biorecognition events trigger an energy transfer process between peptide nanosensors 1 and 2, and the signal from the fluorescent dye decreases.

are designed to interact independently but in close proximity of each other, allowing the generation of a strong FRET signal. The use of multiple biorecognition events also increases the specificity of the assay since FRET will only occur when multiple sensors are bound to the same HIV-1 PR molecule.

Our sensors rely on peptide biorecognition elements: short peptide sequences that recognize HIV-1 PR. These peptide sequences are then labeled with fluorescent dye molecules to actuate the detection signal. The position of the interaction between the first peptide sensor and the protease is determined by choosing a known inhibitory peptide sequence of the enzyme (LLEYSL, identified by Lee and Maruyama).[14] Being a competitive inhibitor peptide, it must interact in the active site of the enzyme. A selection of complementary recognition peptides that interact with other regions of the protein was identified through phage display. Phage display is a powerful technique to identify peptide sequences which show an affinity for a particular target. While it has been most successful in identifying sequences which bind inorganic surfaces,[15] it has also been heavily utilized to identify sequences that can have applications in drug discovery[16] and toward the design of synthetic antibody libraries.[17] Phage-display derived peptides have also successfully been used as biorecognition elements in biosensors.[18]

While peptides have an intrinsically lower binding affinity than larger protein molecules such as antibodies[15] on account of their lack of secondary structure, they remain well-suited to their use as protein recognition elements due to their simple chemical structure and ease of synthesis compared to large proteins. They can also be easily incorporated into more complex nanomaterials[19] as they are more stable to harsh environments such as low pH or temperature which can alter the conformation of protein-based materials. This makes them ideal for use in sensing applications, especially with regard to point-of-care diagnostic tools in resource-limited settings.

■ MATERIALS AND METHODS

Experimental Methods. *Enzymes.* Recombinant HIV-1 protease was purchased from BioVendor and used as received. Lyophilized, salt-free pepsin (Sigma-Aldrich) at >2500 units/mg was resuspended in the appropriate assay buffer at 4 mg/mL. Lyophilized Papain (Worthington Biochemicals) was prepared to 20 units/mL in the appropriate assay buffer.

Phage Display. A Ph.D.-7 phage display kit (New England Biolabs) was purchased, and the recommended protocol[20] was followed. In brief, 2.4 μM HIV-1 protease was coated onto the surface of a well of Nunc-Immuno MicroWell 96 well plate in 0.1 M $NaHCO_3$ and left at 4 °C overnight. The well was then washed and blocked with a blocking buffer of 5 mg/mL bovine serum albumin (BSA) in TBS for an hour. After washing to remove bound proteins, 5 μL of the phage library was added to each well in 95 μL Tris buffered saline with 0.05% (v/v) Tween-20, pH 7.4 (TBST). The phage was allowed to interact for an hour before nonbound phage was removed through vigorous washing. Bound phage was eluted with 0.2 M glycine-HCl (pH 2.2) including 1 mg/mL BSA. The eluted phage was then neutralized with the addition of 1 M Tris-HCl (pH 9.1) and then added to 20 mL of *E. coli* ER2738 and left to grow for 5 h for amplification. The eluted phage was quantified by plating these *E. coli* on LB XGal/IPTG plates. Since the library phages are derived from the M13mp19 vector, which carries the lacZa gene, phage-infected plaques acquired a blue color when plated on media containing Xgal (5-bromo-4-chloro-3-indoyl-*b*-D-galacto-side) and IPTG (isopropyl-*b*-D-thiogalactoside). Colored plaques were picked, and DNA was sequenced from these plates (sequencing was carried out by GATC Biotech, Germany). Subsequent biopanning rounds were then carried out by applying the eluted and amplified phage to plated HIV-1 protease. Three rounds of biopanning were carried out in this manner.

Peptides. Sensor peptides were synthesized by standard automated Fmoc solid-phase peptide synthesis as described earlier. Synthesis used a Rink-amide solid resin on a PTI Quartet peptide synthesizer. The peptides were cleaved and deprotected with 95:2.5:2.5 trifluoroacetic acid (TFA)/triisopropylsilane/H_2O for 3 h and precipitated and washed with cold diethyl ether. The crude peptides were purified to >95% (determined by LC−MS) on a preparative C_{18} HPLC column using a water/acetonitrile mobile phase containing 1% (v/v) TFA. Biotinylated peptides were purchased at >95% purity from Genscript.

ELISA. Nunc-Immuno MicroWell 96-well solid plates were coated with 1.2 μM HIV-1 protease in 0.1 M $NaHCO_3$ and incubated overnight at 4 °C. BSA was prepared at 1 mg/mL and coated in the same buffer as a control. Wells were then blocked with 2% (w/v) skim milk for 1 h at room temperature and washed well with PBST (0.05% (v/v) Tween-20). Biotinylated peptides, dissolved in PBS with 10% (v/v) DMSO, were then added at 100 μg/mL to each well and left to incubate for 1 h at room temperature. The plate was then washed again in PBST before the addition of streptavidin-linked hydrogen peroxidase and left to incubate for 45 min. The presence of the peptide was quantified by the addition of a tetramethylbenzidine (TMB) colorimetric substrate, and the absorbance at 450 nm was measured.

Inhibition Assay. An assay to measure the inhibition of HIV-1 protease was performed using a fluorogenic substrate of HIV-1 protease,[21] purchased from Sigma-Aldrich. This is a synthetic peptide sequence that contains the HIV-1 PR cleavage site (Tyr-Pro) and two covalently modified amino acids labeled with a FRET pair (EDANS, 5-2(aminoethylamino)-1-napthalenesulfonate and DABCYL, 4,4′-dimethylaminoazobenzene-4-carboxylate). The substrate was prepared in a 500 μM stock solution in dimethyl sulfoxide (DMSO). Assays were performed at room temperature in a buffered solution of 0.1 M sodium acetate, 1.0 M sodium chloride, 1.0 mM ethylenediaminetetraacetic acid (EDTA), 1.0 mM dithiothreitol (DTT), 10% (v/v) DMSO, and 1 mg/mL BSA at pH 4.7. Enzyme and substrate concentrations were kept constant at 240 nM and 10 μM, respectively. Measurements of the intensity at 490 nm were taken over 3 min in a FluoroLog spectrophotometer (Horiba).

Fluorophore-Peptide Labeling. Alexa Fluor 647 was purchased as a succinimidyl ester from Life Technologies. The dyes were dissolved to 1 mg/mL in dimethyl sulfoxide and coupled at a 1:1 ratio with purified peptides including 1 equiv of 1-ethyl-3-(3-(dimethylamino)propyl) carbodiimide (EDC) and 0.2 equiv of 4-dimethylaminopyridine (DMAP). The reaction was left overnight at room temperature. The solution was then diluted 10× into an acidic mobile phase of water/acetonitrile containing 0.1% (v/v) TFA and purified on a semi-

DOI: 10.1021/acs.chemmater.5b03651
Chem. Mater. XXXX, XXX, XXX−XXX

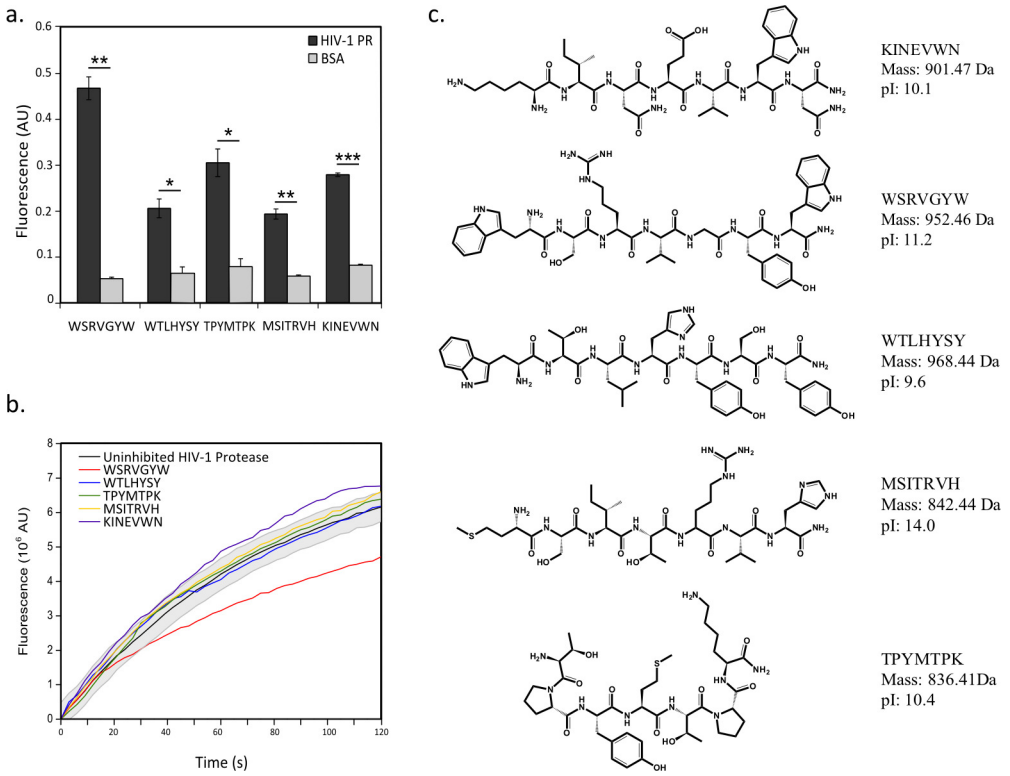

Figure 2. Characterization of five peptide sequences isolated from phage display as potential binders to HIV-1 protease. (a) ELISA showing binding of sequences to HIV-1 protease compared to BSA as a control protein. Error bars shown are standard deviation (n = 3). Significance is given by a two-tailed student t test. * = $p < 0.05$, ** = $p < 0.01$, *** = $p < 0.005$. (b) Competitive inhibition assay of sequences in the presence of a large excess of phage-display peptides (10 μM). The peptide WSRVGYW partially inhibits the enzyme at high concentrations. (c) Amino acid structures of selected peptides.

preparative HPLC using a C_{18} column. Colored fractions were collected and analyzed by UV−vis spectroscopy to identify the single fraction containing peaks at 220 and 280 nm (indicative of the peptide backbone) and 647 nm (corresponding to the Alexa Fluor dye). Peptides conjugated to these dyes were not seen through LC-MS or MALDI as has been reported previously,[22] and a full discussion can be found in the Supporting Information (Figure S9). BHQ-3 as a succinimidyl ester was purchased from Biosearch Technologies and conjugated in the manner described above. Fractions collected after HPLC purification were identified via LC−MS showing an MW of 1443.7 (expected 1410.59, observed mass in positive mode = M + methanol + H^+).

NHS-fluorescein and NHS-rhodamine were purchased from Pierce Biotechnology. The dyes were dissolved in DMSO to 100 mM. The dyes were then added at a 1:1 ratio to the protected peptides on resin. The dyes were allowed to couple overnight at room temperature in dimethylformamide (DMF) with 25 μL of *N,N*-diisopropylethylamine (DIPEA). The peptides were then cleaved from the resin and purified as described above. Fractions collected after HPLC were identified via LC−MS showing an MW of 1093.5 (LLE-fluor, expected: 1094.27, observed mass in negative mode = M − H^+) and 683 (WSR-rhod, expected: 1364.6, observed mass in positive mode = M + $2H^+$).

FRET Surface Assay. Amine functionalized glass slides (Sigma-Aldrich) were immersed in 0.1 M sodium bicarbonate (pH 8.6) with 10% (v/v) glutaraldehyde and left for 1 h. The slides were then washed thoroughly with deionized water before being dried with nitrogen. HIV-1 protease was prepared at 50 μg/mL in 0.1 M sodium bicarbonate with 10 mM sodium cyanoborohydride. A 10 μL portion of the protein solution was spotted onto the preprepared glass slide and left for 3 h in a humidity chamber. The slides were then washed thoroughly with deionized water. Unreacted amines were blocked with a solution of 1 M ethanolamine in 0.1 M sodium bicarbonate with 1% (w/v) BSA (at pH 8.6). The slides were left to block for 1 h and then washed thoroughly. The slide was immersed in WSR-647 for 1 h in the dark before being washed in PBST (0.05% (v/v) Tween-20), before being imaged at 700 nm with a Li-Cor Odyssey infrared scanner. Half the slide was then immersed in LLE-BHQ-3 while the other half was left in PBST for an hour in the dark. The slide was then washed thoroughly with PBST again and reimaged. The intensity of the spots was quantified using Li-Cor Image Studio.

In Solution FRET. LLE-fluor and WSR-rhod at 20 μM were added to varying concentrations of HIV-1 PR in the PR assay buffer described above, adjusted to pH 6 to a final volume of 60 μL in the wells of a 384 clear-bottom black microwell plate. The plate was incubated in the dark at 4 °C for an hour before the fluorescent spectra were read on a SpectraMax M5 plate reader (Molecular Devices). The solution was excited at 480 nm, and the emission was read between 510 and 600 nm with a cutoff value of 495 nm.

Computational Methods. *Structure Preparation.* For the HIV-1 protease, crystal structures with the protease flaps open (PDB ID 2PC0), semiopen (PDB ID 1HHP), and closed (PDB ID 1HVC) were used. Two side chains were changed (I3V and C95A) in 1HHP to match the native protease sequence. For 1HVC, the structural, active-site water molecule, HOH-415, was retained for docking, but all other crystallographic water was removed. Hydrogens were added to the structures using AutoDockTools (ADT) from Autodock 4.2.[23]

Docking. Initial configurations for the peptide−protease complexes were generated using the docking program Autodock 4.2, with default settings used unless otherwise noted. Three overlapping grids were defined on the basis of areas of interest (Supporting Information, Figure S6). WSRVGYW and LLEYSL were used as ligands, with Gasteiger charges assigned by ADT. Each peptide was docked into each grid for the three protease structures, with a maximum of 10 000 000 energy evaluations and 27 000 genetic algorithm generations using the Lamarckian Genetic Algorithm. For each docking run, the top 100 structures based on the Autodock estimation of free energy of binding were examined, and the 3D structures of the top 10 were evaluated for geometric fit variation to select the

DOI: 10.1021/acs.chemmater.5b03651
Chem. Mater. XXXX, XXX, XXX−XXX

distinctive starting structures for subsequent molecular dynamics (MD) simulations.

Molecular Dynamics. MD simulations were performed using the Amber 12 MD code[24] and Amber force field.[25] The systems were solvated with a TIP3P water[26] box extending at least 12 Å from the complex resulting in a box containing approximately 34 000−36 000 atoms. Chloride ions were added to neutralize the overall charge. Asp25 in the catalytic site was protonated to mimic the PR in its native configuration.[27] Bond lengths involving hydrogen were constrained using the SHAKE algorithm.[28] The particle-mesh Ewald scheme was used for the electrostatic interactions, with a nonbond interaction cutoff (electrostatics and van der Waals) of 8 Å.

Prior to dynamics, the systems were minimized using the steepest descent algorithm, followed by a conjugate gradient method, with a convergence criterion of 10^{-4} kcal/mol Å. Position restraints of 2 kcal/mol Å^2 were maintained on the protein and peptide atoms during minimization and equilibration. Equilibration consisted of 50 ps of constant-volume MD as the system was heated from 0 to 300 K, followed by 50 ps of constant pressure MD. Unrestrained simulations of up to 20 ns were performed for each system, with atomic coordinates saved every 10 ps. A 2 fs time step was used. Temperature was maintained at 300 K by a Langevin thermostat, and pressure was maintained at 1 atm by a Berendsen barostat.

■ RESULTS AND DISCUSSION

To identify peptide sensor 1, phage display was carried out against immobilized HIV-1 PR. A Ph.D.-7 phage-display library from New England Biolabs containing approximately 10^{11} clones of 10^9 individual sequences was incubated against the target protein. Three rounds of biopanning were carried out, and enrichment was observed (Supporting Information, Figure S1). Some 32 clones were then selected for sequencing and were then assessed for binding to HIV-1 PR. Binding was established through an enzyme-linked immunosorbent assay (ELISA) against the M13 bacteriophage, and from this, five candidates were selected and sequenced. These were then f2 synthesized and further characterized (Figure 2). Through an ELISA-like enzyme linked binding assay utilizing biotinylated peptides, all five candidates showed preferential binding to HIV-1 PR compared to an immobilized control protein (bovine serum albumin, BSA). A competitive inhibition assay was then used to determine whether any of the peptides altered the proteolytic activity of HIV-1 PR, in order to determine whether they interacted near to the active site of the peptide, where peptide sensor 2 is located (Figure 1). The FRET signal between peptide sensors 1 and 2 is distance dependent, and therefore peptides interacting in the vicinity of the active site may result in the highest FRET efficiency. One of the sequences (WSRVGYW) shows mild inhibitory effects with a K_i of 229 μM (Supporting Information, Figure S2).

Given the single active site of the protease, the competitive inhibition shown in Figure 2b implies that WSRVGYW must interact in the vicinity of the active site. It was thus identified as the most promising sequence found through phage display since it is expected to be positioned close to peptide sensor 2, which should maximize the FRET efficiency. Peptide sensor 1 was fabricated by synthesizing WSRVGYW and conjugating a fluorescent molecule, Alexa Fluor 647 (AF647), to the N-terminus. Peptide sensor 2 was fabricated by synthesizing the inhibitory sequence LLEYSL, to a Black Hole Quencher-3 (BHQ-3), also through the N-terminus. Both sensors form a FRET pair in which BHQ-3 acts as a dark quencher for the fluorescent AF647 dye. Thus, if both peptide sensors are simultaneously interacting with a single protease molecule, a decrease in the fluorescence of AF647 should be observed.

HIV-1 PR was immobilized on amine functionalized glass slides using glutaraldehyde coupling. After unreacted groups were blocked, the slide was incubated for an hour with peptide sensor 1 at a concentration of 210 μM. After thoroughly washing the membrane for an hour to remove nonspecifically bound dye, the slide was imaged (Figure 3a). The interaction f3

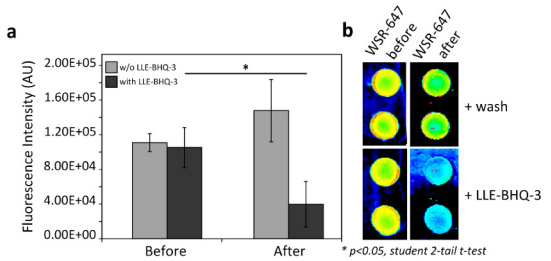

Figure 3. On surface FRET showing detection of HIV-1 PR using two independent recognition events. (a) Quantification of fluorescence quenching on surface. Error bars shown are standard deviation (n = 3). Significance is given by a two-tailed student t test. (b) The presence of immobilized HIV-1 PR can be seen through the fluorescence signal of nanosensor 1 (WSR-AF647). On addition of nanosensor 2 (LLE-BHQ-3) the fluorescence signal is quenched. No such signal decrease is observed through continued washing.

between the peptide sensors 1 and the HIV PR can be clearly observed in Figure 3a. When the slide was incubated with peptide sensor 2 at a concentration of 609 μM, the fluorescent signal was quenched (Figure 3b). The decrease in fluorescence was not seen when the peptide was incubated with a nonlabeled version of LLEYSL, which demonstrates that it is originated by FRET and not by competition for the biorecognition of the protease (see Supporting Information, Figure S3). This supports the hypothesis that both peptides are binding to the protease giving multiple independent recognition events. Furthermore, when the membrane was incubated in the working buffer, no signal decrease was observed, which demonstrates that the decrease in fluorescent signal did not originate by washing peptide sensor 1 off the protein (Figure 3b). No FRET was observed when the two peptide sensors were incubated in the absence of HIV-1 PR (Supporting Information, Figure S3). These experiments demonstrate that it is possible to detect HIV PR with the proposed detection scheme based in the dual biorecognition by peptide sensors.

The peptide sensors can detect immobilized HIV-1 PR at the concentration of 800 nM or higher (Supporting Information, Figure S4). This concentration value is likely dictated by the K_{off} of the WSR peptide (K_d = 44.6 μM). The binding affinity of the LLEYSL peptide is much stronger (K_d = 3.04 nM), and hence, the sensitivity of the assay will lie between these two values (Supporting Information, Figure S5). Peptides found through phage display are well-known for displaying low to moderate binding affinity.[15]

We next performed molecular dynamics (MD) simulations in order to ascertain whether it would be possible for both peptides to interact with the enzyme's active site simultaneously, giving rise to the observed FRET signal and to confirm our design principles.

Initial molecular docking of the inhibitor peptide LLEYSL and the best binding sequence from phage dis-play to the protease was performed using Autodock 4.2[23] in order to identify energetically favorable starting structures of the molecular complexes which were then simulated using classical

DOI: 10.1021/acs.chemmater.5b03651
Chem. Mater. XXXX, XXX, XXX−XXX

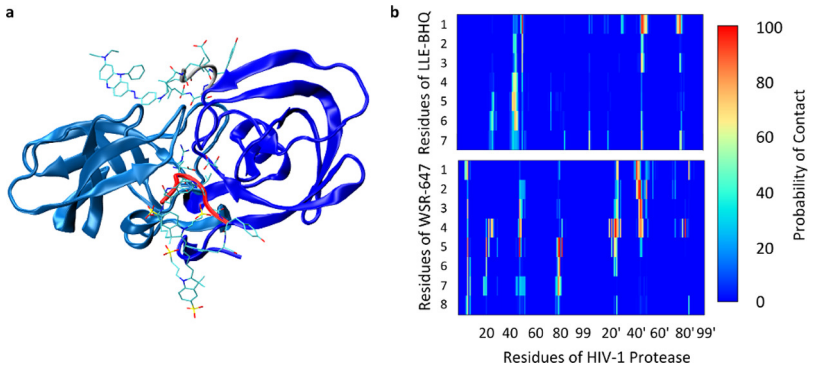

Figure 4. Simulated structure of HIV-1 PR complexed with peptide nanosensors: (a) The most populated cluster from REST simulations showing both peptide−dye conjugates bound to the protease flaps on opposite sides of the active site. WSRVGYW is shown in red, and LLEYSL is shown in green. (b) Contact maps showing the interaction probabilities with HIV-1 PR for each residue of the nanosenors for the most populated cluster of the peptide−dye conjugates. Residue 1 represents the contacts between the dye or quencher to the protease, and the peptides are subsequently numbered from N-terminus to C-terminus.

all-atom molecular dynamics using Amber 12.[24] Three conformations of the protease were used, namely, with its flaps open, semiopen, and closed. For each conformation, three areas were electrostatically mapped to explore interaction areas for the peptides: the active site, the hinge region, and the "bottom" of the enzyme (Supporting Information, Figure S6).

For each peptide/flap/grid combination the top 100 docking orientations were ranked using an estimated free energy of binding, and for each combination the 3D structures of the top 10 best binders were examined. As a result, a total of 15 protein−ligand complexes were chosen for molecular dynamics simulation, on the basis of the docking score, specificity of the docking poses, and ligand contacts with the protease. Some peptide/flap/grid combinations did not yield any complexes with favorable free energy of binding or were not significantly different in peptide backbone position from other docking poses, and thus were not considered for molecular dynamics. Of the 15 peptide−protease complexes simulated, 12 were found to have negative free energies of binding calculated by the MM-PBSA approach. WSRVGYW was found to have a favorable free energy of binding, and bound most strongly in the active site. This is in good agreement with experimental data for WSRVGYW.

Binding of LLEYSL in the active site is characterized by hydrogen bonding of Asp30′and Asp25′ to the Ser side chain and second Leu backbone in the peptide sequence. These bonds are present in all simulations where there was a favorable free energy of binding for this peptide. The strongest predicted binding structures also show hydrophobic interactions between the peptide Tyr and Phe53′. The interaction of WSRVGYW with the active site also shows significant dependence on hydrogen bonding between the N-terminus Trp backbone and Ser side chain with Asp30′. In these simulations, we also observed several hydrophobic interactions between Tyr and the C-terminus Trp with the Phe53 and Phe53′ flap residues, similar to that seen for LLEYSL.

We hypothesized that binding to the hinge region of the protease could have a potential influence on the activity of the enzyme, since an interaction here would prevent the flaps of the enzyme from closing, hence preventing the formation of the catalytic triad required for proteolysis. However, the simulations showed that the binding of both WSRVGYW and LLEYSL in this region was predicted to be orders of magnitude less than in the active site. Binding conformations that originate in the hinge region progressively interacted with the flaps over the course of the simulations. Because of this only a few hydrophobic interactions are observed between the peptides and the Ile residues found in the protease flaps (Ile50, Ile54). This is to be expected given that this is the hydrophilic, solvent-exposed surface of the protease. From these studies it is therefore reasonable to suggest that both WSRVGYW and LLEYSL occupy the active site of HIV-1PR.

The interactions of the peptide sensors with the protease were also simulated to observe the impact of the presence of the dye molecule on the binding. Conformational sampling was performed using the REST (replica exchange with solute tempering) procedure with convergence determined by a plateau in the number of new structures found by the clustering analysis.

Clustering was performed on the two peptide backbones separately with an RMSD cutoff of 1.2 Å over the final 50 ns of the 200 ns REST trajectory (Figure 4a). The most populated clusters found for both WSRVGYW and LLEYSL are structurally similar to their respective conformations obtained from the 800 ns classical molecular dynamics simulations. Both peptides are relatively stable in their binding positions, characterized by the change in free energy as a function of the peptide radial distance from the HIV-1 PR catalytic residues (Supporting Information, Figure S7). An enhanced discussion of the clustering is given in the Supporting Information.

Interestingly, there are similar features between the binding interactions of the two peptides (Figure 4b). Both sensors form a hydrogen bond with the Gly48 backbone of the protease flap, and both have persistent hydrophobic contacts with the hydrophobic pocket formed by Ile50, Val82, Ile84, and Leu23, as well as hydrophobic contacts with Phe53 on the protease flap. The experimentally observed inhibitory action of both peptides may be due to interference with the opening of the flaps rather than occupation of the active site as seen with other inhibitors.[29]

To demonstrate the potential of this technique for one-step diagnostics and to test whether our designed peptide sensors generated a high efficiency signal, the FRET assay was performed with the enzyme free in a buffered solution. In this case the peptides were synthesized with fluorescein and rhodamine conjugated to the N-terminus. These were designated LLE-fluor and WSR-rhod, respectively. This was done to modulate the fluorescence intensity of the rhodamine

DOI: 10.1021/acs.chemmater.5b03651
Chem. Mater. XXXX, XXX, XXX−XXX

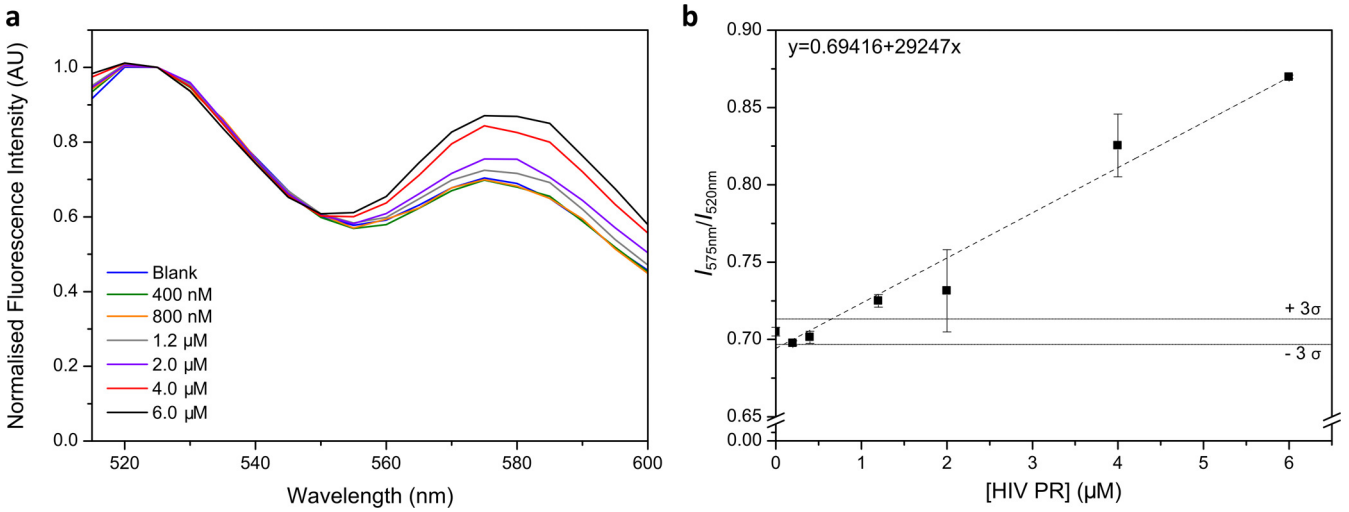

Figure 5. (a) Steady-state emission spectra of FRET in solution showing an increasing fluorescence transfer with increasing concentrations of HIV-1 PR (λ_{ex} = 480 nm) following a 1 h incubation at 4 °C. (b) Variation of the FRET signal with the concentration of HIV PR showing the limit of detection calculated as 3σ.

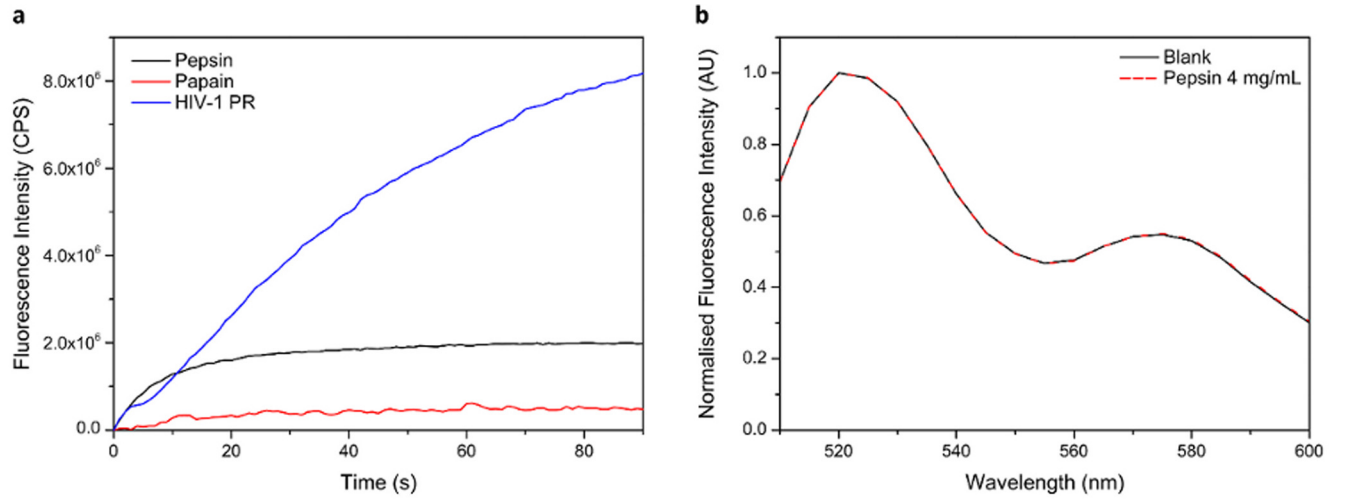

Figure 6. Comparison of assay specificity using different enzymes: (a) The commercial HIV-1 substrate shows some vulnerability to nonspecific cleavage by pepsin, an aspartyl protease but not to enzymes from a different family. (b) The assay developed here shows no response to an excess of pepsin when compared to the blank control.

which is highly pH dependent and more sensitive to cross-excitation at lower pH.[30] At this pH the protease is less active but not conformationally affected since its high pI means it is most stable between pH 4 and 6.[31] HIV-1 PR was incubated with both peptide sensors at a concentration of 20 μM (LLE-fluor and WSR-rhod) for 1 h in the dark at 4 °C. The assay was incubated in the cold in order to slow the K_{off} rate of the peptides and thus improve the assay's sensitivity.

The FRET assay has a limit of detection of 654 nM calculated as the concentration of analyte that yields a signal higher than 3 times the standard deviation on the blank, 3σ (Figure 5). This is in good agreement with the lowest concentration which is observable by eye in the immobilized experiments (Supporting Information, Figure S4). In order to understand the low limit of detection observed for this assay, the FRET efficiency was calculated using time correlated single photon counting spectroscopy (TCSPC) in the presence of 4 μM HIV-1 PR (Supporting Information, Figure S8).

The fluorescence lifetime of the donor molecule (fluorescein) in the presence and absence of the acceptor (rhodamine) was measured. In the absence of the acceptor, a single exponential gives a lifetime of 3.92 ns. In the presence of the acceptor the data follows a single-exponential yielding a decay of 3.53 ns. From this, using eq 1 where τ_D is the donor fluorescence in the absence of acceptor and τ_{DA} is the fluorescence of the donor in the presence of an acceptor, we can calculate an efficiency of only 9.95%.

$$E = 1 - \frac{\tau_{DA}}{\tau_D} \quad (1)$$

This low efficiency could be explained by several factors. First, it is possible that WSR-rhod is interacting with the enzyme further from the active site than is predicted by the models above (the simulations suggest a center-of-mass to center-of-mass distance between the two dye molecules of 2.68 (±0.27) nm). Second there is likely a dominant effect of the high k_{off} of WSR-rhod.

DOI: 10.1021/acs.chemmater.5b03651
Chem. Mater. XXXX, XXX, XXX−XXX

Although we do not see two populations in the lifetime measurements that would indicate the presence of an unquenched population, the low rate of energy transfer may mask this effect. Since the concentration of WSR-rhod used in this assay is below the K_D of the peptide we can assume that at this concentration only 30.9% of PR molecules are labeled with an acceptor, while >99.98% of molecules will be labeled with a donor molecule.

Calculating a distance between a FRET pair is difficult with such a low efficiency since the r^6 dependence becomes insensitive to changes above the Förster distance. Differences between the calculated distance from the FRET studies (7.60 nm) and that expected from the MD may also arise due to the different structure of the dye molecules which act as a reporter probe (AF647/BHQ-3 vs fluorescein/rhodamine) which may affect the calculated binding orientation, leading to differences in center-of-mass distances. Other differences may occur due to variations of the orientation factor (κ is assumed to be $^2/_3$ when the dyes are free to rotate). Differences in this value would impact the Förster radius used to calculate the dye−dye distance. The use of rhodamine as an acceptor dye can also introduce errors to this calculation due to its broad absorption spectrum and hence significant direct excitation.

A major advantage of the proposed detection strategy compared to classical approaches based on cleavable peptide substrates is the high specificity of the detection due to the multiple interaction events. In a conventional assay, proteases with similar specificity to the target protease can also cleave peptides with FRET pairs leading to false positives. Our test does not rely on substrate cleaving and requires two independent biorecognition events, which increases the specificity of the assay. To prove the specificity of the proposed detection scheme, the assay was repeated using pepsin. Pepsin is the most ubiquitous of the aspartyl proteases and demonstrates a broad substrate recognition.

Pepsin at the manufacturer's recommended working concentration of 4 mg/mL was incubated at pH 2 (the optimal pH for pepsin activity) with the commercial HIV-1 protease substrate used for inhibition studies above. This acts as a model system of a FRET pair linked through a cleavable peptide substrate.

f6 Figure 6a shows that the commercial system is vulnerable to nonspecific cleavage since it yields a positive signal in the presence of pepsin. The enzyme papain, a cysteine protease, is included as a control from a different enzymatic family to show that substrates are usually vulnerable to nonspecific enzymes from structurally similar enzymes. In comparison, Figure 6b shows the same concentration of pepsin (at large excess) incubated with the peptide sensors. The experimental conditions are identical to those used for the in-solution FRET assay described above. In this instance, no difference can be observed between the blank and the pepsin therefore confirming our hypothesis that using two peptide sensors results in highly specific signals.

CONCLUSIONS

We have demonstrated that HIV-1 protease, a critical enzyme in the lifecycle of HIV/AIDS, can be detected through designed interactions with multiple peptide sensors. This approach to biomarker detection requires two independent binding events, a strategy that improves the specificity of the assay. Our methodology is also differentiated from other protease-based assays in that the signal is not dependent on proteolytic cleavage which can be susceptible to nonspecific enzymes. We also remove the need for the multiple wash steps that are required with conventional ELISA assays, streamlining the laboratory process. While the affinity of the peptide sensor found through phage display to HIV-1 PR is lower than would be expected from an antibody, we believe the advantages in environmental stability and length scale make these sensors well-suited to FRET applications. Through molecular dynamics simulations we have explored the interaction between the protease and the peptides to understand the mechanisms which cause these binding events and developed a model for the simultaneous binding of both peptide sensors to HIV-1 protease. It is hoped that our assay will provide a new direction for the design of highly specific protein sensing without the need for costly antibody development.

ASSOCIATED CONTENT

Supporting Information

The Supporting Information is available free of charge on the ACS Publications website at DOI: 10.1021/acs.chemmater.5b03651.

Additional figures showing supporting data, details about calculations, and supporting methods details (PDF)

AUTHOR INFORMATION

Corresponding Authors

*Contact for modeling details. E-mail: irene.yarovsky@rmit.edu.au.

*Contact for experimental details. E-mail: m.stevens@imperial.ac.uk.

Present Address

[§]Department of Pure and Applied Chemistry, University of Strathclyde, 295 Cathedral Street, Glasgow G1 1XL, United Kingdom.

Author Contributions

All authors have given approval to the final version of the manuscript.

Funding

The RMIT Foundation International Research Exchange Fellowship is gratefully acknowledged for providing funds for research exchange visits between Imperial College London and RMIT University, Melbourne (K.-L.H). Australian Research Council Discovery Grant DP 140101888 (I.Y. and M.M.S.) is acknowledged. M.M.S. acknowledges EPSRC grant EP/K020641/1 and the ERC Seventh Framework Programme Consolidator Grant "Naturale CG" under grant agreement no. 616417.

Notes

The authors declare no competing financial interest.

ACKNOWLEDGMENTS

The authors thank Dr. Lisa Haigh (Department of Chemistry, Imperial College London) for assistance with mass spectrometry, Dr. Simon Burbidge of the Imperial College High Performance Computing Centre for conversations regarding these simulations, Dr. Nadav Amdursky (Imperial College London) for assistance with TCSPC measurements, and Dr. Philip Howes (Imperial College London) and Dr. Nevena Todorova (Health Innovations Research Institute, RMIT University) for useful discussions. We acknowledge the generous allocation of high performance computational

DOI: 10.1021/acs.chemmater.5b03651
Chem. Mater. XXXX, XXX, XXX−XXX

resources from the Australian National Computational Infrastructure (NCI), the Western Australian Computational Facility (iVEC), the Victorian Partnership for Advanced Computing (VPAC), and the Victorian Life Sciences Computational Initiative (VLSCI).

■ ABBREVIATIONS

EDC, 1-ethyl-3-(3-(dimethylamino)propyl)carbodiimide; NHS, *N*-hydroxysuccinimide; EDANS, 5-2-(aminoethylamino)-1-napthalenesulfonate; DABCYL, 4,4′-dimethylaminoazobenzene-4-carboxylate; HPLC, high pressure liquid chromatography; BHQ-3, black hole quencher-3; AF647, Alexa Fluor 647; HIV-1 PR, human immunodeficiency virus-1 protease; AIDS, auto immune deficiency syndrome; FRET, Förster resonance energy transfer; Xgal, 5-bromo-4-chloro-3-indoyl-*b*-D-galactoside; IPTG, isopropyl-*b*-D-thiogalactoside; TMB, tetramethylbenzidine; TFA, trifluoroacetic acid; DMF, dimethylformamide; DIPEA, *N*,*N*-diisopropylethylamine; MM-PBSA, molecular mechanics-Poisson−Boltzmann surface area; REST, replica exchange with solute tempering

■ REFERENCES

(1) World Health Organisation, Global Summary of the AIDS Epidemic 2013, 2014, accessed online http://www.who.int/hiv/data/en/.

(2) Navia, M. A.; Fitzgerald, P. M.; McKeever, B. M.; Leu, C. T.; Heimbach, J. C.; Herber, W. K.; Sigal, I. S.; Darke, P. L.; Springer, J. P. Three-dimensional Structure of Aspartyl Protease from Human Immunodeficiency Virus HIV-1. *Nature* **1989**, *337*, 615−620.

(3) Pokorná, J.; Machala, L.; Rezáčová, P.; Konvalinka, J. Current and Novel Inhibitors of HIV Protease. *Viruses* **2009**, *1*, 1209−1239.

(4) Mahmoud, K. A.; Hrapovic, S.; Luong, J. H. Picomolar Detection of Protease Using Peptide/Single-Walled Carbon Nanotube/Gold Nanoparticle-Modified Electrode. *ACS Nano* **2008**, *2*, 1051−1057.

(5) Mahmoud, K. A.; Luong, J. H. A Sensitive Electrochemical Assay for Early Detection of HIV-1 Protease Using Ferrocene-Peptide Conjugate/Au Nanoparticle/Single Walled Carbon Nanotube Modified Electrode. *Anal. Lett.* **2010**, *43*, 1680−1687.

(6) Choi, Y.; Lee, J.; Kim, K.; Kim, H.; Sommer, P.; Song, R. Fluorogenic Assay and Live Cell Imaging of HIV-1 Protease Activity Using Acid-Stable Quantum Dot-Peptide Complex. *Chem. Commun. (Cambridge, U. K.)* **2010**, *46*, 9146−9148.

(7) Esseghaier, C.; Ng, A.; Zourob, M. A Novel and Rapid Assay for HIV-1 Protease Detection Using Magnetic Bead Mediation. *Biosens. Bioelectron.* **2013**, *41*, 335−341.

(8) Wong, E. Y.; Hewlett, I. K. HIV Diagnostics: Challenges and Opportunities. *HIV Ther.* **2010**, *4*, 399−412.

(9) Suaifan, G. A.; Shehadeh, M.; Al-Ijel, H.; Ng, A.; Zourob, M. Recent Progress in Prostate-Specific Antigen and HIV Proteases Detection. *Expert Rev. Mol. Diagn.* **2013**, *13*, 707−718.

(10) Cornett, J. K.; Kirn, T. J. Laboratory Diagnosis of HIV in Adults: A Review of Current Methods. *Clin. Infect. Dis.* **2013**, *57*, 712−718.

(11) Medintz, I. L.; Clapp, A. R.; Brunel, F. M.; Tiefenbrunn, T.; Uyeda, H. T.; Chang, E. L.; Deschamps, J. R.; Dawson, P. E.; Mattoussi, H. Proteolytic Activity Monitored by Fluorescence Resonance Energy Transfer Through Quantum-Dot-Peptide Conjugates. *Nat. Mater.* **2006**, *5*, 581−589.

(12) Lowe, S. B.; Dick, J. A. G.; Cohen, B. E.; Stevens, M. M. Multiplex Sensing of Protease and Kinase Enzyme Activity *via* Orthogonal Coupling of Quantum Dot-Peptide Conjugates. *ACS Nano* **2012**, *6*, 851−857.

(13) Ghadiali, J. E.; Lowe, S. B.; Stevens, M. M. Quantum-dot-Based FRET Detection of Histone Acetyltransferase Activity. *Angew. Chem., Int. Ed.* **2011**, *50*, 3417−3420.

(14) Lee, T. G.; Maruyama, S. Isolation of HIV-1 Protease-Inhibiting Peptides from Thermolysin Hydrolysate of Oyster Proteins. *Biochem. Biophys. Res. Commun.* **1998**, *253*, 604−608.

(15) Artzy-Schnirman, A.; Abu-Shah, E.; Dishon, M.; Soifer, H.; Sivan, Y.; Reiter, Y.; Benhar, I.; Sivan, U. On the Limited Recognition of Inorganic Surfaces by Short Peptides Compared with Antibodies. *J. Pept. Sci.* **2014**, *20*, 446−450.

(16) Molek, P.; Strukelj, B.; Bratkovic, T. Peptide Phage Display as a Tool For Drug Discovery: Targeting Membrane Receptors. *Molecules* **2011**, *16*, 857−887.

(17) Lee, C. V.; Liang, W.-C.; Dennis, M. S.; Eigenbrot, C.; Sidhu, S. S.; Fuh, G. High-Affinity Human Antibodies from Phage-Displayed Synthetic Fab Libraries with a Single Framework Scaffold. *J. Mol. Biol.* **2004**, *340*, 1073−1093.

(18) Qi, H.; Qiu, X.; Xie, D.; Ling, C.; Gao, Q.; Zhang, C. Ultrasensitive Electrogenerated Chemiluminescence Peptide-Based Method for the Determination of Cardiac Troponin I Incorporating Amplification of Signal Reagent-Encapsulated Liposomes. *Anal. Chem.* **2013**, *85*, 3886−3894.

(19) de la Rica, R.; Matsui, H. Applications of Peptide and Protein-Based Materials in Bionanotechnology. *Chem. Soc. Rev.* **2010**, *39*, 3499−3509.

(20) Ph.D. Phage Display Libraries, New England Biolabs, accessed online, June 2015, https://www.neb.com/~/media/Catalog/All-Products/A597C3819D8F421782485716A5AB8AD2/Datacards%20or%20Manuals/manualE8102.pdf.

(21) Matayoshi, E.; Wang, G. T.; Krafft, G. A.; Erickson, J. Novel Fluorogenic Substrates for Assaying Retroviral Proteases by Resonance Energy Transfer. *Science* **1990**, *247*, 954−958.

(22) Esteban, A.; Popp, M. W.; Vyas, V. K.; Strijbis, K.; Ploegh, H. L.; Fink, G. R. Fungal Recognition is Mediated by the Association of Dectin-1 and Galectin-3 in Macrophages. *Proc. Natl. Acad. Sci. U. S. A.* **2011**, *108*, 14270−14275.

(23) Morris, G. M.; Huey, R.; Lindstrom, W.; Sanner, M. F.; Belew, R. K.; Goodsell, D. S.; Olson, A. J. AutoDock4 and AutoDockTools4: Automated Docking With Selective Receptor Flexibility. *J. Comput. Chem.* **2009**, *30*, 2785−2791.

(24) Case, D.; Darden, T.; Cheatham, T., III; Simmerling, C.; Wang, J.; Duke, R.; Luo, R.; Walker, R.; Zhang, W.; Merz, K. *AMBER 12*; University of California, San Francisco, 2012.

(25) Lindorff-Larsen, K.; Piana, S.; Palmo, K.; Maragakis, P.; Klepeis, J. L.; Dror, R. O.; Shaw, D. E. Improved Side-Chain Torsion Potentials For The Amber Ff99sb Protein Force Field. *Proteins: Struct., Funct., Genet.* **2010**, *78*, 1950−1958.

(26) Silva, A. M.; Cachau, R. E.; Sham, H. L.; Erickson, J. W. Inhibition And Catalytic Mechanism Of HIV-1 Aspartic Protease. *J. Mol. Biol.* **1996**, *255*, 321−346.

(27) Jorgensen, W. L.; Chandrasekhar, J.; Madura, J. D.; Impey, R. W.; Klein, M. L. Comparison Of Simple Potential Functions For Simulating Liquid Water. *J. Chem. Phys.* **1983**, *79*, 926−935.

(28) Ryckaert, J.-P.; Ciccotti, G.; Berendsen, H. J. C. Numerical Integration Of The Cartesian Equations Of Motion Of A System With Constraints: Molecular Dynamics Of N-Alkanes. *J. Comput. Phys.* **1977**, *23*, 327−341.

(29) Wensing, A. M. J.; van Maarseveen, N. M.; Nijhuis, M. Fifteen years of HIV Protease Inhibitors: raising the barrier to resistance. *Antiviral Res.* **2010**, *85*, 59−74.

(30) Sjöback, R.; Nygren, J.; Kubista, M. Absorption and Fluorescence Properties of Fluorescein. *Spectrochim. Acta, Part A* **1995**, *51*, L7−L21.

(31) Szeltner, Z.; Polgar, L. Conformational Stability and Catalytic Activity of HIV-1 Protease Are Both Enhanced at High Salt Concentration. *J. Biol. Chem.* **1996**, *271*, 5458−5463.

DOI: 10.1021/acs.chemmater.5b03651
Chem. Mater. XXXX, XXX, XXX−XXX